

Structural relaxation effects on interface and transport properties of Fe/MgO(001) tunnel junctions

Xiaobing Feng, O. Bengone, and M. Alouani

Institut de Physique et Chimie des Matériaux de Strasbourg,
UMR 7504 CNRS-ULP, 23 rue du Loess, Strasbourg 67034, France

S. Lebègue

Laboratoire de Cristallographie et de Modélisation des Matériaux
Minéraux et Biologiques UMR UHP-CNRS 7036, Nancy, France

I. Rungger and S. Sanvito

School of Physics and CRANN, Trinity College, Dublin 2, Ireland

The interface structure of Fe/MgO(100) magnetic tunnel junctions predicted by density functional theory (DFT) depends significantly on the choice of exchange and correlation functional. Bader analysis reveals that structures obtained by relaxing the cell with the local spin-density approximation (LSDA) display a different charge transfer than those relaxed with the generalized gradient approximation (GGA). As a consequence, the electronic transport is found to be extremely sensitive to the interface structure. In particular, the conductance for the LSDA-relaxed geometry is about one order of magnitude smaller than that of the GGA-relaxed one. The high sensitivity of the electronic current to the details of the interface might explain the discrepancy between the experimental and calculated values of magnetoresistance.

Tunnel magneto-resistance (TMR) is the change of the electric resistance of a magnetic trilayer made of two ferromagnetic metallic electrodes separated by an insulating spacer, when the mutual orientation of the electrodes' magnetizations changes from parallel alignment (PA) to antiparallel alignment (AA). The figure of merit for the effect is the TMR ratio, defined as

$$\text{TMR} = \frac{G_{\text{PA}} - G_{\text{AA}}}{G_{\text{AA}}},$$

where G_{PA} (G_{AA}) is the conductance for the PA (AA) configuration. Among the possible material combinations Fe/MgO(100) magnetic tunnel junctions (MTJs) have attracted much attention, since extremely large TMR ratios were theoretically predicted on the basis of symmetry-driven spin filtering from the tunnel barrier¹. These have been now demonstrated experimentally^{2,3,4} and the symmetry filtering effect is now widely accepted. However, the measured TMR ratios are usually significantly lower than those predicted by *ab initio* methods.

The origin of such a discrepancy is currently a matter of debate. On the theory side, interface resonance states (IRSs) located around the Fermi energy (E_{F}) are important for the zero-bias transport⁵ and are usually difficult to describe accurately. Moreover the MgO band-gap is significantly underestimated by LSDA and GGA, so that the barrier height might not be accurately predicted. On the experimental side, the quality of Fe/MgO MTJs depends on the preparation methods. The 4% lattice mismatch between Fe and MgO produces dislocations and significant relaxation at the interface. In addition, in typical growth conditions the Fe layers close to the interface might be partially oxidized.⁶

Several different geometries for the Fe/MgO interface have been proposed theoretically, based on relaxing $[\text{Fe}]_n/[\text{MgO}]_m$ supercells, consisting of n Fe and m

MgO monolayers (MLs) subject to various constraints. In Ref. [1] LSDA relaxation for a $[\text{Fe}]_5/[\text{MgO}]_5$ superlattice, in which the in-plane lattice constant is held at the LSDA value for bulk Fe, yields a Fe-O distance of 2.17 Å. In contrast an early LSDA calculation for one Fe ML on MgO substrate predicted an Fe-O distance of 2.3 Å.⁷ Likewise a GGA study for one MgO ML on a Fe slab returns a Fe-O distance of 2.21 Å, and a separation between the first and the second Fe ML 6% smaller than that of bulk Fe.⁸ How relevant calculations for single MLs on surfaces are for Fe/MgO MTJ is however not clear and there is still disagreement between experiments⁹ and theory⁷. These controversies over the correct interface structure bring the question of how the different interface geometries affect the electronic and transport properties. Our Letter aims at answering this question.

We perform structural relaxations for a $[\text{Fe}]_{10}/[\text{MgO}]_6$ superlattice with both the LSDA and GGA¹⁰ functionals by means of the PAW method¹¹ as implemented in the VASP code¹². Charge transfer and magnetic moments are calculated for the differently relaxed structures with Bader analysis¹³ using the LSDA densities. A 12×12 in-plane \mathbf{k} -point grid and an energy cutoff of 400 eV are employed to converge the charge density. As benchmark we find for bulk Fe a lattice constant of 2.75 Å and a bulk modulus of 2.68 Mbar, both in good agreement with other all-electron LSDA calculations.¹⁴ Then, the transport properties are computed with the SMEAGOL¹⁵ code, which combines the non-equilibrium Green's functions (NEGF) formalism with DFT.¹⁶ The GGA PBE¹⁷ functional and a 400×400 \mathbf{k} -point grid are used for calculating the transmission coefficient.

The layer spacings at the Fe/MgO interfaces obtained after structural relaxation are summarized in Tab. I. These have been obtained by keeping fixed the in-plane lattice constant, set equal to the experimental value for

DFT	d_{-4}	d_{-3}	d_{-2}	d_{-1}	d_0	d_1	d_2	d_3
Unrelaxed	1.433	1.433	1.433	1.433	2.160	2.026	2.026	2.026
LSDA	1.297	1.313	1.343	1.120	2.002	2.130	2.119	2.119
GGA	1.380	1.414	1.427	1.350	2.219	2.199	2.177	2.185

TABLE I: (Color online) The interface structure of a $[\text{Fe}]_{10}/[\text{MgO}]_6$ superlattice obtained by LSDA and GGA relaxation. The structural parameters for the unrelaxed structure are taken from Ref. [1]. The middle two Fe layers are frozen at a separation of 1.43 Å and the experimental lattice constant for bulk Fe is used for the in-plane lattice constant. d_n indicates the separation (in Å) between layers from Fe/MgO the surface ($n = 0$), with the index $n > 0$ ($n < 0$) labels MgO (Fe) layers.

Fe, and the atomic position of the two most internal Fe MLs. In the table we report the obtained layer spacings along the stack direction d_n , where d_0 represents the Fe-O distance at Fe/MgO interface and $n > 0$ ($n < 0$) refers to separation between MgO (Fe) MLs. In the table we also report the unrelaxed structural parameters taken from reference¹.

LSDA relaxation gives a Fe-O distance of 2.0 Å. This is significantly different from 2.16 Å of the unrelaxed structure. The LSDA relaxation also predicts that the spacing, d_{-1} , between the first two Fe layers next to the Fe/MgO interface is drastically reduced to 19% of that of bulk Fe. The changes in layer spacing of the MgO barrier on the other hand are relatively small. Interestingly, the GGA results are significantly different from the LSDA ones. In particular, GGA returns a Fe-O distance of 2.22 Å and the reduction of d_{-1} is less pronounced than that for the LSDA. Our GGA-relaxed structure is in good agreement with other GGA studies^{8,18} and rather close to the reference unrelaxed interface structure.

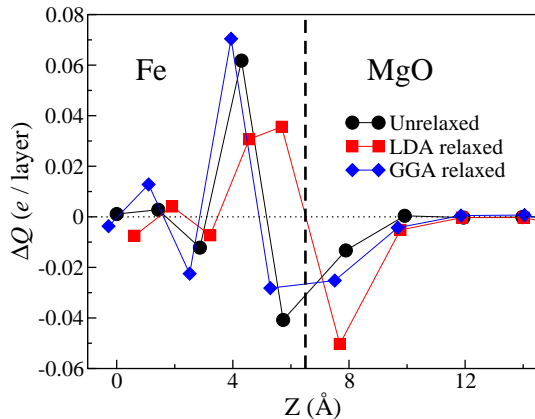


FIG. 1: (Color online) Charge transfer, ΔQ , for a $[\text{Fe}]_{10}/[\text{MgO}]_6$ superlattice as calculated from Bader analysis. Net charge transfer is obtained by subtracting the atomic charges of bulk Fe and bulk MgO from the Bader atomic charges in the Fe/MgO superlattice. The vertical dashed line denotes the Fe/MgO interface.

Fig. 1 demonstrates that the charge transfer between Fe and MgO is very sensitive to the interface structure. The Bader analysis for the LSDA-relaxed geometry predicts that the first two Fe MLs at the Fe/MgO interface

acquire a similar amount of electron charge, ΔQ , while for the GGA-relaxed and unrelaxed structures it indicates that the interface Fe ML loses electrons and the second Fe ML gains a significant amount of charge. In all cases MgO loses electrons to Fe. Similar charge transfer from MgO to neighboring metallic layers was predicted before for Rh/MgO interfaces.¹⁹ For the LSDA-relaxed structure we predict a net electron transfer from MgO to Fe of up to about 0.06 electrons per atom. This is larger than the one for the other two geometries. The Bader charges for O atoms at the interface and in the middle of the MgO barrier are respectively 7.64 and 7.71. This indicates that charge is transferred to Fe mainly from O. Finally, since the GGA-relaxed structure is close to the unrelaxed one, the charge transfer is also similar.

The local magnetic moments of the Fe atoms [Fig. 2(a)] are calculated by integrating the spin densities in the domains determined by charge densities resulting from the Bader analysis. These are similar for the GGA-relaxed and unrelaxed structures, both presenting a significant enhancement of the Fe magnetic moment at the MgO interface. For the LSDA-relaxed structure however such interfacial magnetic moment is dramatically suppressed. This is only 1.10 μ_B , to be compared with 2.65 μ_B and 2.68 μ_B respectively for the GGA-relaxed and unrelaxed geometries. Since ΔQ is much smaller than the change in the magnetic moment, the dramatic decrease of interface magnetic moment in the LSDA calculations is caused by an internal electron redistribution between the majority and minority spin sub-bands. This is demonstrated by the spin-decomposed electron occupation [Fig. 2(b)]. Since in the LSDA relaxation d_{-1} is significantly shorter than that for GGA relaxation, the suppression of the magnetic moment is expected, based on the fact that many magnetic materials undergo magnetic collapse under pressure.²⁰

The effects of the interface structure on the electronic transport are studied with SMEAGOL.¹⁵ At zero bias the conductance, G , is simply $G = e^2/h T(E_F)$, where e is the electron charge, h the Planck's constant and $T(E_F)$ the transmission coefficient calculated at E_F . $T(E_F)$ is presented in Fig. 3. The transmission for majority spins in the PA depends weakly on the energy but it is reduced by about one order of magnitude for the LSDA-relaxed structure, when compared to both the GGA and the unrelaxed ones. In contrast the minority spin chan-

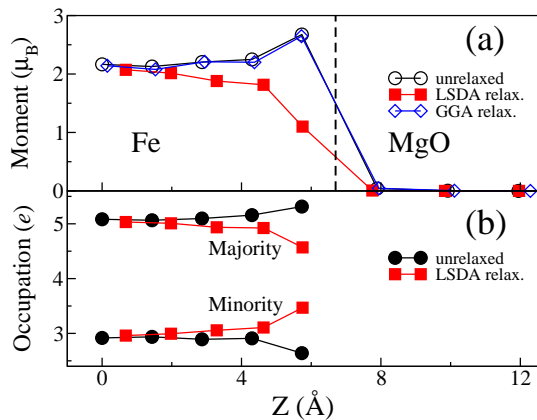


FIG. 2: (Color online) The magnetic moment (a) and spin-decomposed electron occupation (b) for a $[\text{Fe}]_{10}/[\text{MgO}]_6$ superlattice. These are calculated using Bader analysis for the valence electrons. The vertical dashed line in the top panel denotes the Fe/MgO interface.

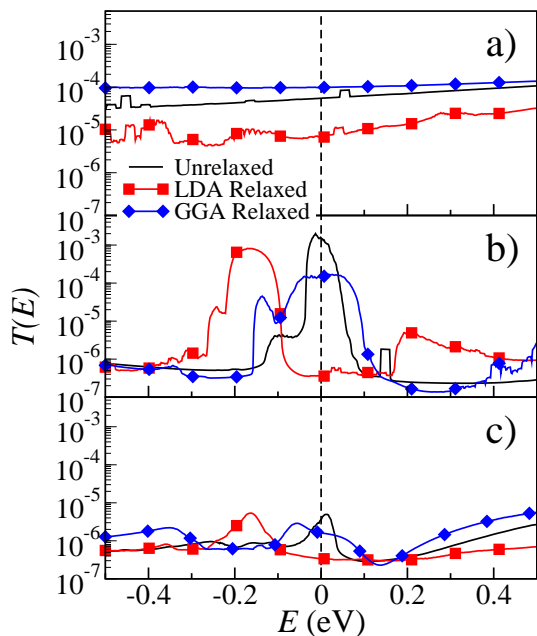


FIG. 3: (Color on line) Transmission $T(E)$ for PA majority spins (a), PA minority spins (b), and for the AA (c) of a Fe/MgO/Fe MTJ. The Fermi energy is set to zero.

nel for PA is dominated by a peak at around E_F . This originates from IRSs at the Fe/MgO interface.²¹ For the LSDA-relaxed structure these peaks are shifted 0.2 eV to lower energies with respect to the GGA-relaxed case. A similar shift is found for both spins in the AA configuration. This shift leads to a large change in the low bias conductance. As is shown in Tab. II, the total conductance of the LSDA-relaxed structure is about 30 times smaller than that of GGA-relaxed structure for the PA. Although the magnetic moment and charge transfer are similar for the GGA-relaxed structure and the unrelaxed

structure, the transmission coefficients for the two structures are significantly different. The GGA-relaxed structure shows less pronounced and wider peaks in the transmission coefficient than those of the unrelaxed structure. This results in the conductance of GGA-relaxed structure being 5 times smaller than that of the unrelaxed one.

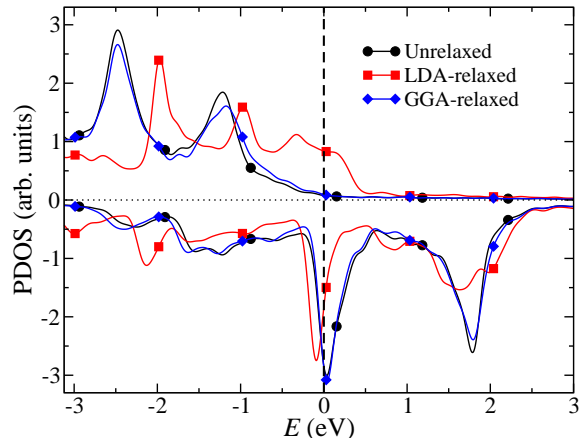


FIG. 4: (Color on line) The projected density of states of the interface Fe 3d orbitals in a $[\text{Fe}]_{10}/[\text{MgO}]_6$ junction. Positive and negative projected DOS represent the majority and minority components, respectively.

Since the peak in transmission at around E_F originates from the IRSs at the Fe/MgO interface, the shift in energy of the transmission coefficient for the LSDA-relaxed structure relative to that of the GGA-relaxed one is the result of a high sensitivity of IRSs to the interface geometry. In Fig. 4 the density of states (DOS), projected on the interface Fe layer, is shown for both spins. For the LSDA-relaxed structure this is shifted by about 0.2 eV with respect to that of the GGA-relaxed structure, which causes the corresponding energy shift of $T(E)$. Since the unrelaxed and GGA-relaxed structures are close to each other, the general features of the projected DOS for the two are also similar. In order to get a better insight into the role of relaxation, in Fig. 5 we show the \mathbf{k} -resolved projected DOS at E_F for the interfacial Fe layer. The results for the unrelaxed and GGA-relaxed structures are rather similar, but they differ remarkably from that for the LSDA-relaxed case. In general the LSDA-relaxed geometry shows a substantial reduction of the spin-polarization, demonstrated by the fact that the \mathbf{k} -resolved DOS is similar for the majority and minority spins. This is expected to produce a reduction in spin-filtering and as a consequence a reduction in TMR. It is also important to note that the main differences between LSDA-relaxed and GGA-relaxed (and unrelaxed) geometries are more evident around Brillouin zone center, i.e. for electrons with a large linear momentum perpendicular to the MgO barrier and therefore with a larger transmission probability.

The changes in conductance lead to very different values for the TMR. Our calculated values for the TMR

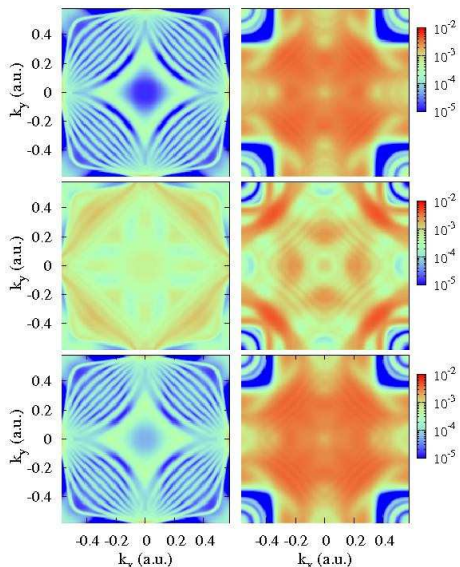


FIG. 5: (Color on line) The \mathbf{k} -resolved projected density of states for the interface Fe ML in a Fe/MgO/Fe junction. Unrelaxed, LSDA-relaxed and GGA-relaxed structures are shown in the top, middle and bottom panels respectively. The left and right panels are for majority and minority spins, respectively.

TABLE II: The TMR and zero bias conductance for PA and AA a Fe/MgO/Fe MTJ. GGA PBE is used for all transport calculations. The results are shown for the unrelaxed, the LSDA-relaxed and for the GGA-relaxed structures. The experimental TMR is for a Fe/MgO/Fe MTJ with a 2.3 nm thick MgO barrier and a temperature of 20 K.³

	G_{PA}	G_{AA}	TMR(%)
unrelaxed	1.21×10^{-3}	7.18×10^{-6}	17,300
LSDA relax.	7.32×10^{-6}	6.74×10^{-7}	986
GGA relax.	2.38×10^{-4}	3.23×10^{-6}	7,270
Expt.	-	-	247

are shown in Tab. II. The LSDA-relaxed structure has a TMR of about 10^3 , which is much smaller than the TMRs of the other two structures, and in much closer agreement to experiments.³ The dramatic reduction of TMR for the LDA-relaxed structure originates from two features: the shift to lower energies of the IRSs transmission peak, and the large reduction of the majority spin transmission for PA. These can be both associated with a loss of spin-polarization of the first Fe layer at the Fe/MgO interface in the LSDA-relaxed case.

In conclusions, motivated by the significant difference between theory and experiments on the reported TMR values in Fe/MgO/Fe(100) MTJs, we studied the interface structure and its effects on the electronic and transport properties by means of DFT and the NEGF formalism. In general LSDA- and GGA-relaxed interfacial geometries are rather different, yielding different charge transfer and interfacial magnetism. In particular the local magnetic moment of the interfacial Fe ML is severely suppressed for the LSDA-relaxed structure and enhanced for GGA-relaxed ones. These differences are reflected in the transport properties. In particular the differences at the interface determine the energy position of resonances in the transmission for the minority spins. These resonances are caused by IRSs and largely determine the zero-bias conductance. As a consequence the TMR is rather sensitive to the interfacial structure. These features can partially explain the disagreement between theory and experiments and are expected to apply to many other systems relevant for spintronics

X.F, O. B, M.A., and S.L acknowledge an ANR grant ANR-06-NANO-053, and I.R and S.S thank Science Foundation of Ireland for financial support (grant nr. 07/IN.1/I945 and 07/RFP/PHYF235).

¹ W. H. Butler, X.-G. Zhang, T. C. Schulthess, and J. M. MacLaren, Phys. Rev. B **63**, 054416 (2001).
² M. Bowen, V. Cros, F. Petroff, J.-M. de Teresa, L. Morellón, M.R. Ibarra, F. Güell, F. Peiró, A. Cornet, and A. Fert, Appl. Phys. Lett. **79**, 1655 (2001).
³ S. Yuasa, T. Nagahama, A. Fukushima, R. Suzuki, and K. Ando, Nature Materials **3**, 868 (2004).
⁴ F. Greullet, C. Tiusan, F. Montaigne, M. Hehn, D. Halley, O. Bengone, M. Bowen, and W. Weber, Phys. Rev. Lett. **99**, 187202 (2007).
⁵ I. Rungger, O.N. Mryasov and S. Sanvito, arXiv:0808.0902 (2008).
⁶ M. Müller, F. Matthes, and C. M. Schneider, Europhysics Lett. **80**, 17007 (2007).
⁷ C. Li and A. J. Freeman, Phys. Rev. B **43**, 780 (1991).

⁸ B. D. Yu and J.-S. Kim, Phys. Rev. B **73**, 125408 (2006).
⁹ T. Urano, J. Phys. Soc. Jpn. **57**, 3403 (1988).
¹⁰ J. P. Perdew, in *Electronic Structure of Solids 91*, edited by P. Ziesche and H. Eschrig (Akademie Verlag, Berlin, 1991), p. 11.
¹¹ P. E. Blöchl, Phys. Rev. B **50**, 17953 (1994).
¹² G. Kresse and J. Hafner, Phys. Rev. B **47**, 558 (1993).
¹³ R. Bader, *Atoms in Molecules: A Quantum Theory* (Oxford University Press, New York, 1990).
¹⁴ E. G. Moroni, G. Kresse, J. Hafner, J. Furthmüller, Phys. Rev. B **56**, 15629 (1997).
¹⁵ A. R. Rocha, V. M. Garcia-Suarez, S. Bailey, C. Lambert, J. Ferrer, and S. Sanvito, Phys. Rev. B **73**, 085414 (2006).
¹⁶ J. M. Soler, E. Artacho, J. D. Gale, A. Garcia, J. Junquera, P. Ordejón, and D. Sanchez-Portal, J. Phys.: Condens.

- Matter **14**, 2745 (2002).
- ¹⁷ J.P. Perdew, K. Burke and M. Ernzerhof, Phys. Rev. Lett. **77**, 3865 (1996).
- ¹⁸ D. Wortmann, G. Bihlmayer, and S. Blügel, J. Phys.: Condens. Matter **16**, S5819 (2004).
- ¹⁹ C. W. M. Castleton, S. Nokbin, and K. Hermansson, Journal of Physics: Conference Series **100**, 082027 (2008), URL <http://stacks.iop.org/1742-6596/100/082027>.
- ²⁰ J. Kunes, A. V. Lukoyanov, V. I. Anisimov, R. T. Scalettar, and W. E. Pickett, Nature Materials **7**, 198 (2008).
- ²¹ I. Rungger, A. R. Rocha, O. Mryasov, O. Heinonen, and S. Sanvito, J. Magn. Magn. Mater. **316**, 481 (2007).